Comparative proteomic analysis of sporulation associated protein SCO4114 in *Streptomyces coelicolor*

Lifen Li[1, 2, 3], Dongmei Liang[1, 2, 3], Ruiqi Chen[1, 2, 3], Guofeng Zhang[1, 2, 3], Edwina Nelson[1, 2, 3], Jianjun Qiao[1, 2, 3], Qinggele Caiyin[1, 2, 3, *]

[1]School of Chemical Engineering and Technology, [2]Key Laboratory of Systems Bioengineering (Ministry of Education), Tianjin University, Tianjin 300072, China. [3]SynBio Research Platform, Collaborative Innovation Center of Chemical Science and Engineering (Tianjin), Tianjin 300072, China.

Received: April 4, 2019; **accepted:** May 8, 2019.

Streptomyces coelicolor **are Gram-positive bacteria with a complex life cycle and produce a variety of secondary metabolites, occupying about 70% of the currently known antibiotics. Its morphological differentiation is closely related to secondary metabolism, so the research on morphological differentiation related regulation mechanism has always been a hot spot. SCO4114 was proposed to be a sporulation associated protein of the *S. coelicolor* A3(2), although the regulation on the growth of aerial mycelium is not clear. In order to better understand the functions of SCO4114 and find out the effects of SCO4114 on aerial mycelium formation at the protein level, the proteomic analysis of *S. coelicolor* A3(2) wild-type (WT) and *sco4114* deletion (*Δsco4114*) strains were conducted by combining iTRAQ labeling and LC-MS analysis. Total of 2,996 proteins were identified, of which 163 were significantly differentially expressed. Due to the iTRAQ-based quantitative proteomics approach, it was indicated that important metabolic pathways such as carbohydrate metabolism, energy metabolism, fatty acid metabolism, amino acid metabolic pathways, purine and pyrimidine metabolism were involved in regulation and expression of proteins. The metabolic pathways also included replication, transcription, translation, and cell walling synthesis, membrane transport, and signal transduction. Based on the analysis of proteomic data, we speculated that knockout of *sco4114* gene affect the formation of aerial mycelium by affecting the primary metabolic process of *Streptomyces* and the stable expression of *bld* system. The present study is comprehensive proteomic analysis of *S. coelicolor* strain and it provides some clues to understand the sporulation mechanism of *S. coelicolor*.**

Keywords: *Streptomyces coelicolor*; quantitative proteomics; differentially expressed proteins; sporulation; morphological differentiation.

***Corresponding author:** Qinggele Caiyin, 135 Yaguan Road, Jinnan District, Tianjin 300350, China. Phone: +86 22 2740 3389. E-mail: qinggele@tju.edu.cn.

Introduction

Streptomyces coelicolor, as a model strain of *Streptomyces*, has complicated processes of morphological differentiation and physiological metabolism, and can produce a great deal of secondary metabolites [1]. The main metabolites, such as the aromatic polyketide antibiotic actinorhodin (ACT) and the tripyrolle antibiotic undecylprodigiosin (RED) and so on, were produced by *S. coelicolor* A3(2).

The morphological differentiation process of *S. coelicolor* is very complicated, mainly including the spores of *Streptomyces* absorb water and nutrients, expand and germinate, and gradually form mycelium in the base. After the mycelium develops to a certain stage, it grows into aerial mycelium. Then the aerial mycelium develops to form spore filaments and sporangia on the top, and finally develops into spores. Most regulators that govern the transitions between these stages

in life cycle of *S. coelicolor* have been investigated and validated [2-8].

It has been indicated that this regulation consists of a variety of gene systems and transcriptional regulatory factors, including *bld* gene system, *whi* gene system, *ram* gene system, *ssg* gene system, and *chaplins* gene system etc. The *bld* gene system controls the development node of *Streptomyces* aerial mycelium when all the external environmental conditions and physiological and biochemical indicators in the bacteria reach the developmental node of the growth of aerial mycelium. The *bld* gene system can induce the expression of surfactant *sapB* and *chaplins* proteins, and drive the formation of aerial mycelium [9, 10]. The *whi* gene system is composed of multiple genes, among which, *whiB* gene transcription produces cysteine-rich transcription factors, playing a significant part in the formation of *Streptomyces* spores [11]. The *ram* gene system can promote the rapid formation of *Streptomyces* aerial mycelium [12]. The *ssg* gene system is related to the formation of spore septum and spore abscission of *Streptomyces* [13]. The *chaplins* gene system is composed of eight genes designated as *chpA*, *chpB*, *chpC, chpD*, *chpE*, *chpF*, *chpG*, *chpH,* all of which are related to the formation of aerial mycelium of *Streptomyces* [14]. It is important to study the mechanism of morphological differentiation of *Streptomyces* for the industrial production of antibiotics.

In the process of industrial production of various antibiotics, the unlimited proliferation of *Streptomyces* can easily lead to the formation of an excessive density of mycelia, which will affect the normal growth of bacteria, reduce the antibiotic production, and increase the difficulty of product separation [15]. At the same time, the excessive proliferation of bacteria will also affect the flow of medium and oxygen, and consume a lot of nutrients and energy, resulting in limited growth of bacteria and enzyme activity [16].

Mutants that block the aerial mycelium formation are designated as bald phenotype because their colonies lack the hairy appearance characteristic of differentiating colonies. Four classes of bald mutants of *Streptomyces griseus* were identified by Babcock and Kendrick [17]. Among them, the sporulation of class IIIC mutants could be restored by *orf1590*, the highly similar *sco4114* counterpart in *S. griseius* [18]. Accordingly, SCO4114 is considered to be a sporulation associated protein of the model strain *S. coelicolor* A3(2) but the mechanism of SCO4114 in regulating the growth of aerial mycelium is still unclear [18]. By constructing *sco4114* knockout strain (*Δsco4114*), we found that the vegetative growth of the knockout strain was not influenced, but the formation of aerial mycelium was repressed, showing a bald phenotype. Therefore, it can be concluded that SCO4114 controlled the morphological differentiation of *S. coelicolor* from the substrate mycelium into the aerial mycelium [18]. Differential expression patterns of the *Δsco4114* and WT strains of the *S. coelicolor* proteome were obtained by iTRAQ combined with LS-MS. The results shown that the majority of the identified differential proteins involved in carbon metabolism, transcription and translation machinery, protein folding, and amino acid biosynthesis were down-regulated. The proteins involved in coenzyme and inorganic ion transport were up-regulated. Through the analysis of proteomic data, we attempt to explore the role of SCO4114 in the differentiation mechanism of *Streptomyces*.

Materials and Methods

Strains and growth conditions

S. coelicolor M145 strain (WT) and *⊿sco4114* strains were used in this study. YEME liquid medium was used for protein expression and growth curve determination, MS solid culture for colony phenotype observation. All colonies were cultured at 30°C.

Constructing *sco4114* knockout system in *S. coelicolor* M145

CRISPR technology was used to knock out *sco4114* gene. We designed the corresponding sgRNA. The constructed pKCcas9dO plasmids were transferred into *E. coli* ET12567/pUZ8002, and after that they were transferred into *S. coelicolor* M145 through conjugation transduction. Correct conjugant was obtained by resistance screening and PCR verification. Strains of WT and ⊿*sco4114* were inoculated in MS solid medium and cultured at 30℃. The phenotypes were observed (Figure 1A and 1B).

Scanning electron microscopy (SEM)

The wild-type and the mutant colonies of the aerial mycelium grew up on MS agar plates for 72 hours and were observed through scanning electron microscopy. The polymer samples containing the fixed bacteria were immersed in a fixative solution (PBS, 2% glutaraldehyde, and 4% paraformaldehyde) for 15 min and then washed in phosphate-saline buffer solution (PBS). The samples were dehydrated with ethanol solution with gradient concentration (including 50%, 70%, 80%, 90%, 95%) for 15 min at each concentration and then treated twice with anhydrous ethanol for 20 min at each time [19]. The samples were then fixed with a mixture of ethanol and isoamyl acetate (V:V = 1:1) for 15 minutes. Each sample was freeze-dried, sputter-coated with gold, and examined by SEM (S-4800, HITACHI, Japan).

Protein preparation for iTRAQ

Samples extraction was conducted by Lysis buffer 3 (8 M Urea, 40 mM Tris-HCl or TEAB, pH 8.5) including 1 mM PMSF and 2 mM EDTA (final concentration). After placing on ice for 5 min, 10 mM DTT (final concentration) was added to the samples [20]. The suspension was sonicated at 200 W for 1 min and then centrifuged under 4℃, 25 ,000 g for 20 min. The supernatant was incubated under 56℃ for 1 h. Subsequently, the sample was cooled to room temperature and was incubated with 55 mM IAM (final concentration) for 45min in the dark room for alkylation. The supernatant containing proteins was quantified by Bradford method after centrifuge at 25 ,000 g for 20 min at 4℃ [21].

Protein Quantitation with Bradford Assay [22] was performed by adding 0, 2, 4, 6, 8, 10, 12, 14, 16, and 18 µl of BSA (0.2 µg/µl) solution separately to a 96-well plate, and then adding 20, 18, 16, 14, 12, 10, 8, 6, 4, and 2 µl pure water to the corresponding wells. 20 µl of each series diluted unknown sample was added to each well. Then 180 µl of Coomassie Blue was added to each well and mix. The absorbance at OD_{595} of each standard and sample well was read. There were two or more duplicates for each sample. The relationship between the absorbance and the concentration of the standard was plotted, and the extinction coefficient and the concentrations of the unknown samples were calculated.

SDS-PAGE

15-30 µg proteins with loading buffer were mixed in centrifuge tube and heated at 95℃ for 5 minutes [20]. After centrifugation at 25,000 g for 5 minutes, the supernatants were loaded to sample holes on 12% polyacrylamide gel. SDS-PAGE was run under the constant voltage of 120V for 120 minutes. The gel was stained with Coomassie Blue for 2 hours after electrophoresis, and then was de-stained with 40% ethanol and 10% acetic acid.

The protein solution (100 ug) with 8 M urea was diluted 4 times with 100 mM TEAB solution. Protein was digested in proportion by Trypsin Gold (Promega, Madison, WI, USA) at 37℃ overnight with the ratio of trypsin to protein was about 40:1. After trypsin digestion, a Strata X C18 column (Phenomenex) was used to desalt the peptides, and vacuum drying was conducted following the manufacturer's protocol [23].

Peptide labeling and fractionation

The peptides were dissolved in 30 ul of 0.5 M TEAB with vortexing. The reagents were recovered to ambient temperature after the ITRAQ labeling [24] and were transferred and combined with proper samples. Peptide labeling was conducted by ITRAQ Reagent 8-plex Kit. The labeled peptides with varied reagents were

combined and desalted with a Strata X C18 column and then vacuum-dried [23].

Shimadzu LC-20AB HPLC Pump system and a high pH RP column were used to separate the peptides which were reconstituted with buffer A (5% ACN, 95% H_2O, pH 9.8) to 2 ml and were loaded onto a column including 5-µm particles. The process of peptides separation was firstly at a flow rate of 1 ml/min with a gradient of 5% buffer B (5% H_2O, 95% ACN, pH 9.8) for 10 min, then with 5-35% buffer B for 40 min, and 35-95% buffer B for 1 min. The system was then kept in 95% buffer B for 3 min and decreased to 5% within 1 min before equilibrating in 5% buffer B for 10 min. Elution was monitored by measuring absorbance at OD_{214}. The fractions were collected per minute. The eluted peptides were pooled as 20 fractions and vacuum dried [23].

HPLC and mass spectrometer detection

Each fraction was re-suspended in buffer A (2% ACN and 0.1% FA in water) and centrifuged at 25,000 g for 10 min. The supernatant was loaded onto a C18 trap column at 5 µl/min for 8 min through a LC-20AD nano-HPLC instrument by the autosampler. The peptides were eluted from trap column and separated by an analytical C18 column (inner diameter 75 µm) packed in-house. The gradient was run at 300 nl/min starting with 8%~35% buffer B (2% H_2O and 0.1% FA in ACN) in 35 min, and then increased to 60% in 5 min, followed by retained at 80% B for 5 min, and finally returned to 5% in 0.1 min and equilibrated for 10 min [23].

Mass Spectrometer Detection

Data acquisition was conducted with Triple TOF 5600 System equipped with Nanospray III source with a pulled quartz tip as the emitter and controlled by software Analyst 1.6. Data was acquired with the various MS conditions such as ion spray voltage 2,300 V, curtain gas of 30, nebulizer gas of 15, and interface heater temperature of 150°C. High sensitivity mode was used for the whole process of data acquisition and the details could be referred to reference [23].

Statistical analysis and protein identification

The raw MS/MS data was converted into MGF format and exported. The MGF files were searched using the Protein Identification Software Mascot against to the selected database. One or more unique peptide was necessarily required for the identified protein. Automated software IQuant [25] was used to quantitatively analyze the labeled peptides with isobaric tags. Mascot Percolator, a great machine learning method, was integrated to re-score the search results from database and to provide measurements of confidence. In order to evaluate the confidence of peptides, the peptide-spectrum matches (PSMs) were pre-filtered at a PSM-level false discovery rate (FDR) of 1% [23, 26]. Based on the simple principle (or parsimony principle), the sequences of identified peptide were assembled into a set of confident proteins. In order to control the rate of false-positive at protein level, a protein FDR at 1% (based on the picked protein FDR strategy) will also be evaluated after protein inference (Protein-level FDR is not greater than 1%).

Quantitative Real-Time PCR Assay

Total RNA was extracted with ZR RNA MiniPrep. The RNA was reverse transcribed into first-strand cDNA with RevertAid First Strand cDNA Synthesis Kit. The qPCR reactions were performed in 20 µl volume consisting of 5 µl of cDNA (100 ng), 10 µl of LightCycler 480 SYBR Green I Master Mix, 1 µl of each primer, and 3 µl of RNase-Free water. The PCR program ran as follows: preincubation at 95°C for 5 min followed by 45 cycles of 95°C for 10 s, 55°C for 10 s, and 72°C for 20s. For acquisition mode, a melting curve cycle of 95°C for 5 s, 65°C for 1 min, and 97°C was employed. The 16S rRNA gene was the endogenous control gene used for normalization. Triplicate technical replicates were carried out. The differences in the relative expression levels were calculated by the $2^{-\Delta\Delta CT}$ method. The primers used for quantitative real-time (qRT) PCR are shown in Table 1.

Table 1. Primers of genes validation used in qRT-PCT.

Sense primer	Primer sense (5'-3')	Anti-sense primer	Primer sense (5'-3')
sco1947-F	ATGACTCGCATCGGCATCA	sco1947-R	TCAGAGCTGGTTGCCGACG
sco5423-F	ATGCGCCGTTCGAAAATCG	sco5423-R	TCAGCCGCGCCGTGTCT
sco4809-F	ATGGCTATCTGGCTCAACAAGGA	sco4809-R	TCAGCCGGCCAGGATGGC
sco4808-F	GTGGACCTGTTCGAGTACCAGGC	sco4808-R	TTACTTGGCGGCGGCGTG
sco5459-F	ATGACCGTACATCTCGAAGTCG	sco5459-R	TCAGAGGAACGTGGCCTTG
sco2491-F	ATGACCGGCTGGAGCACG	sco2491-R	TCAGGGCAGCAGCGCCTC
sco5477-F	GTGACTACCCAACGCACC	sco5477-R	TTACTTCTTGGGGTTCTTCAGA
sco1476-F	GTGTCCCGTCGCCTGTTCACCT	sco1476-R	TTACAGGCCCGCGGCCTC

Results and Discussion

Effect of *sco4114* gene on aerial mycelium formation

In order to verify the function of SCO4114, *Δsco4114* strain was obtained by CRISPR/Cas9 system. The aerial mycelium formation was inhibited, and only bald colonies could be formed in knockout strain (Figure 1A). To more fully characterize the morphological phenotype of the *⊿sco4114* strain, WT strain and *Δsco4114* strain were cultured on MS solid medium for 72 h, then visualized them by scanning electron microscopy. We found that *Δsco4114* strain couldn't form aerial mycelium, but it entered sporulation stage earlier than WT strain (Figure 1B). Therefore, we suppose that deletion of *sco4114* gene results in pre-maturation of spores. In addition, we measured the growth curves of strains. The results showed that the growth rate of the knockout strain was significantly lower than that of the WT strain (Figure 1C).

Identification and quantification of *S. coelicolor* proteome

In order to explore the effect of *Δsco4114* strain on morphological differentiation in *S. coelicolor*, we set a group of *⊿sco4114*/WT. Under the filter standard of "1% FDR", a total of 2,996 proteins were identified, mainly related to transcription, amino acid metabolism, signal transduction, and carbon metabolism, etc. (Figure 2A). Significantly differential proteins from a single experiment were screened under two conditions including Fold change > 1.2 and Q-value < 0.05. There were 77 significant up-regulated proteins and 86 significant down-regulated proteins in the sample of *⊿sco4114*/WT (Figure 2B).

Analysis of differentially expressed proteins of *Δsco4114* relative to WT

In order to explore the mechanism of SCO4114 protein regulating morphological differentiation, we analyzed the differentially regulated proteins identified at *⊿sco4114*. According to the GOC functional annotation, we analyzed differentially regulated proteins from four aspects including carbon and nitrogen metabolism, ABC transporter system, post-transcriptional modification, and ribosomal proteins.

(a) Carbon and nitrogen metabolism

Most proteins (78.1%) involved in carbon metabolism are significantly down-regulated in *Δsco4114* strain including four proteins involved in glycolysis: fructose diphosphate aldolase (SCO3649), glycerol-3-phosphate hydrogenase (SCO7511 and SCO1947), and pyruvate kinase (SCO5423) (Figure 3A). The majority of the enzymes involved in the citric acid cycle are also significantly down-regulated including citrate

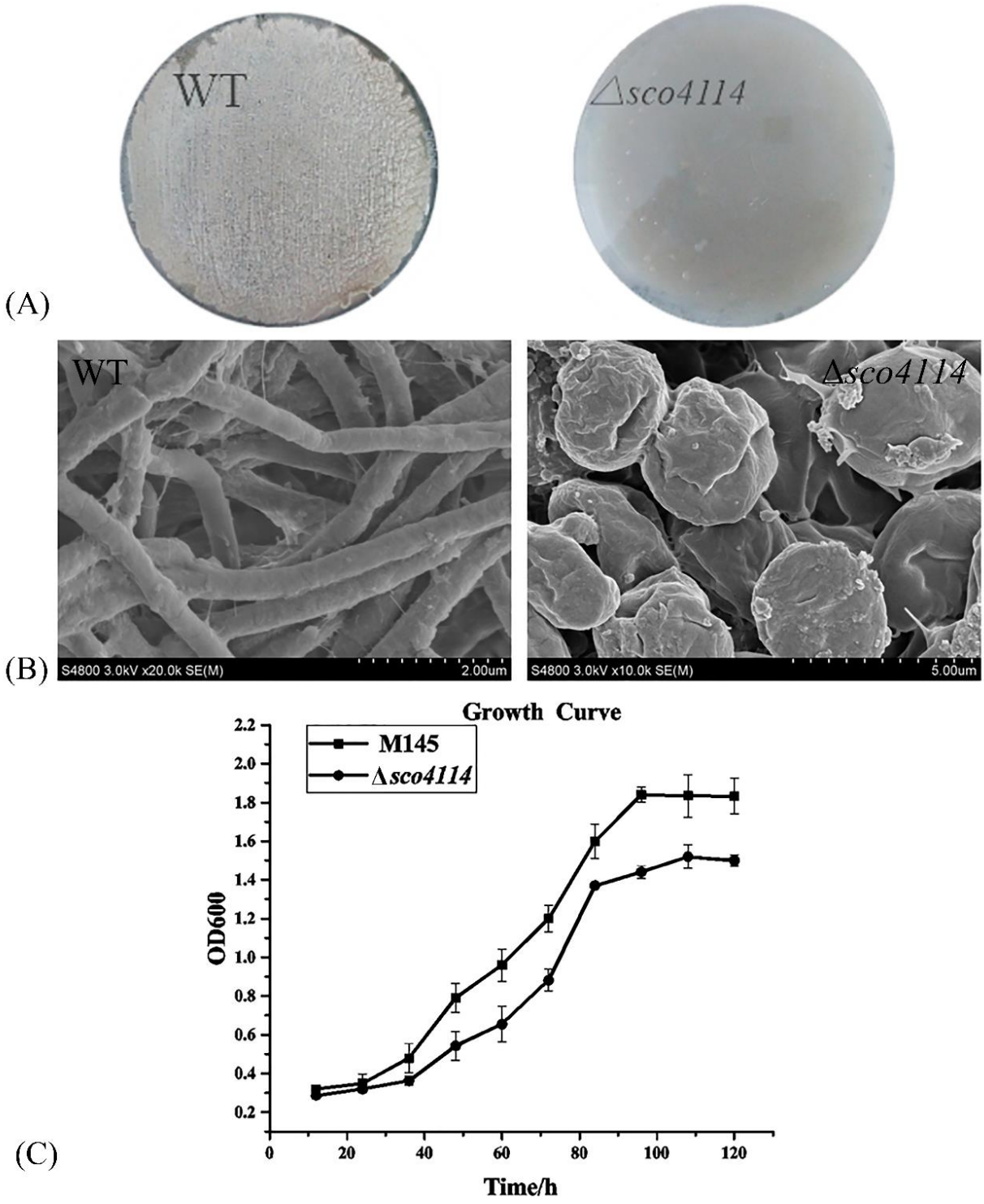

Figure 1. Phenotypic observation and growth curve of wild type and *⊿sco4114* strains. **(A)** The phenotype difference of WT and *⊿sco4114*. Wild-type colonies had obvious aerial hyphae and *⊿sco4114* strains showed bare morphology. **(B)** Morphology of WT and *⊿sco4114* under Scanning Electron Microscope. Left figure showed the mycelium morphology of WT strain. Right figure showed the mold morphology of *⊿sco4114* strain. **(C)** Growth curves of WT and *⊿sco4114* strain. Growth rate of the *⊿sco4114* strain was significantly lower than that of the WT strain.

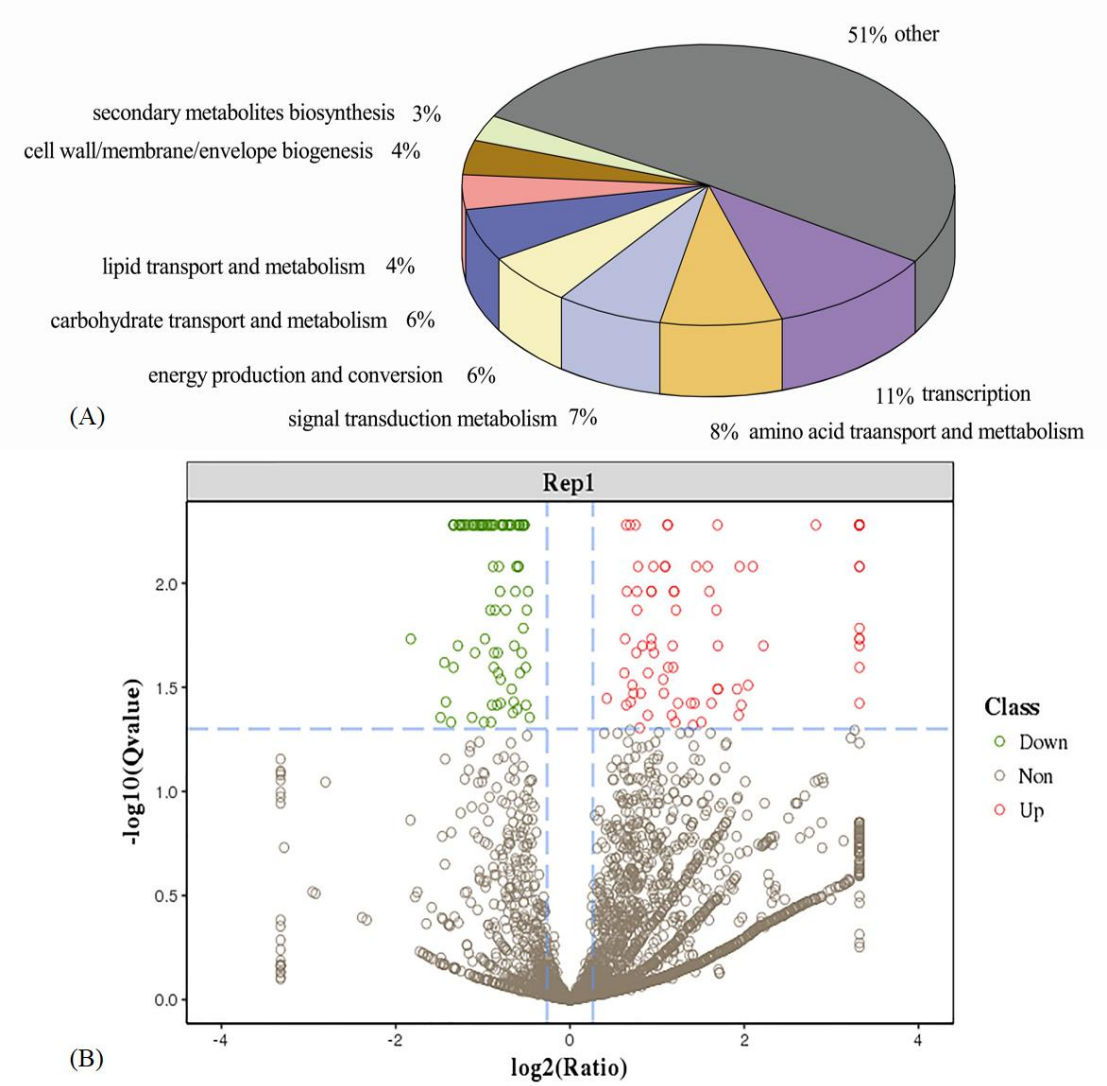

Figure 2. Differentially expressed proteins in *⊿sco4114* compare with WT. **(A)** Classification of the iTRAQ quantified proteins involved in the metabolic pathways. **(B)** Volcano of differentially expressed proteins. The red and green dots were the points-of-interest that showed both large-magnitude fold-changes and high statistical significance. Red dots represented significantly up-regulated proteins which passed screening threshold while green dots indicated significantly down-regulated proteins. Gray dots represented non-significantly differentially expressed proteins.

synthase (SCO2736), aconitase (SCO5999), isocitrate dehydrogenase (SCO7000), and succinyl-CoA synthetase (SCO4809 and SCO4808). It can be seen that the carbon metabolism is slowed down in the *⊿sco4114* strain.

In the *Streptomyces*, carbon catabolite repression (CCR) is considered as the most remarkable control mechanism of physiological processes [27]. This mechanism regulates the expression of genes involved in the uptake and utilization of alternative carbon sources. It also influences the synthesis of secondary metabolites and morphological differentiation [28]. Rapid glucose metabolism can interfere with the synthesis of many compounds and delays morphological differentiation. Therefore, in *⊿sco4114* strain, the slowdown of glycolysis and TCA cycle metabolism may affect the process of morphological differentiation leading to early sporulation.

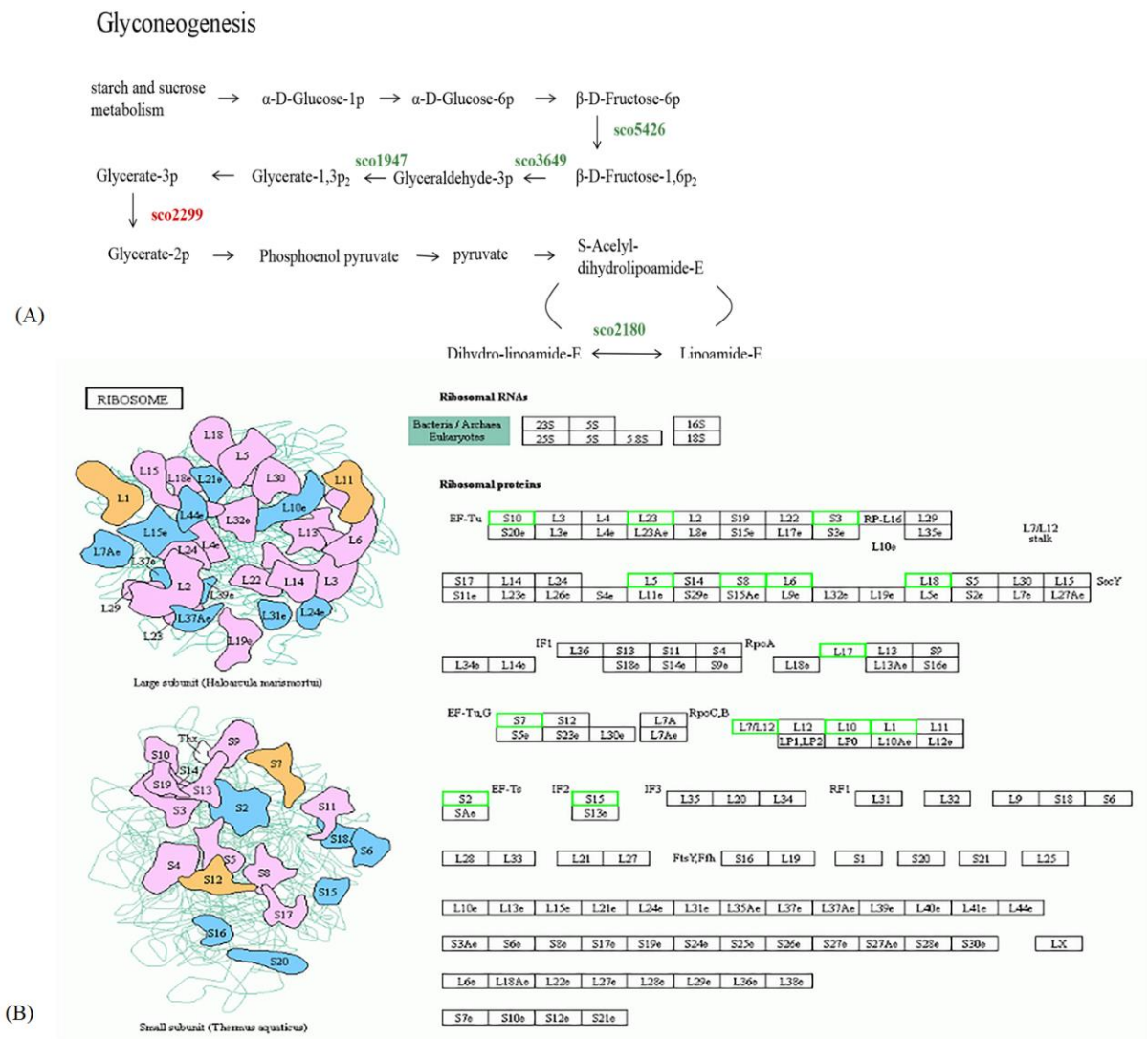

Figure 3. Differentially expressed proteins involved in glycometabolism and ribosome metabolism. **(A)** Integrated proteome data onto a simplified glyconeogenesis metabolic pathway. The genes presented in green were significantly down-regulated in *Δsco4114* strain while those presented in red were significantly up-regulated. **(B)** Significantly down-regulated ribosomal proteins of the small subunit and large subunit. The green box marked with down-regulated proteins.

In addition, expansion pressure is one of the driving forces of aerial mycelium. The concentration and expansion of the storage in the aerial mycelium are adjusted by the decomposition and synthesis of the sugar element, etc. [29]. Therefore, the slowing down of carbon metabolism may indirectly affect the synthesis and decomposition of glycogen in mycelium, which in turn influences the growthof aerial mycelium. The enoyl-coenzyme hydratase (SCO5459) and oxidoreductase (SCO2491) involved in lipid metabolism is up-regulated in *Δsco4114* strain. The lipid decomposition products are also involved in the formation of swelling pressure. When glycolysis and citrate pathway metabolism slow down, lipid metabolism is accelerated to compensate for the expansion pressure required for the growth of aerial mycelium.

(b) ABC transporter system

Most of the proteins (81.8%) involved in amino acid metabolism are down-regulated. Among them, oligopeptide-binding protein (SCO5477)

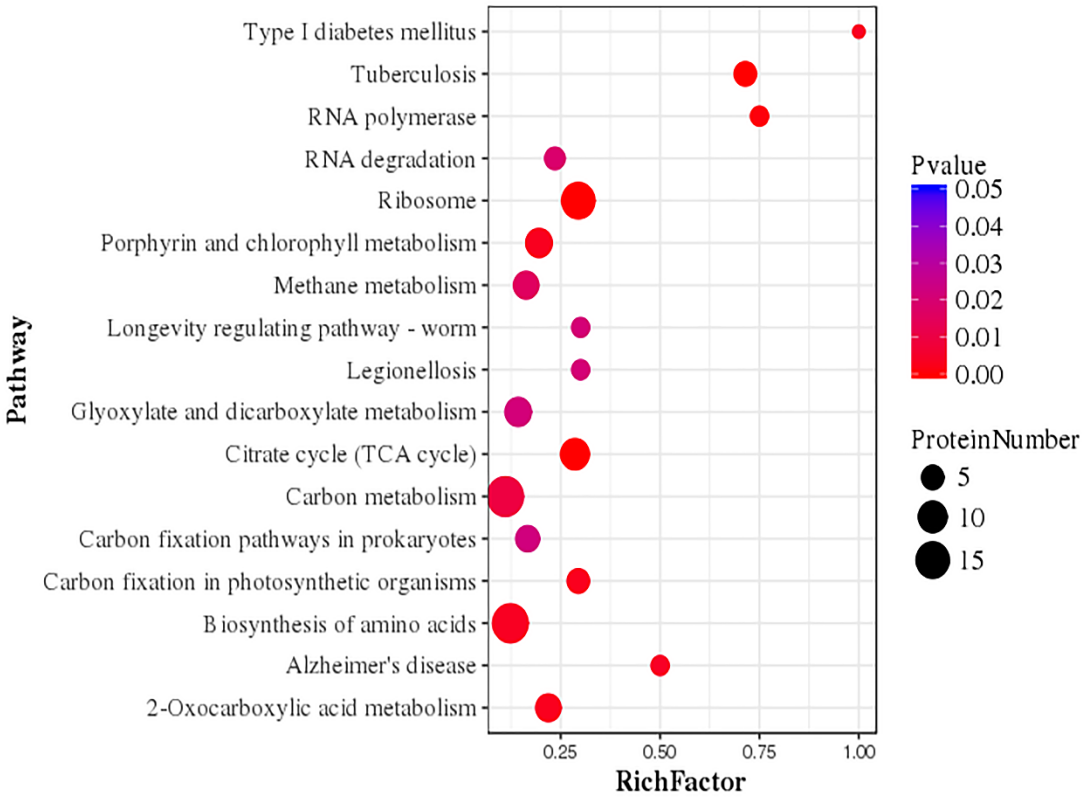

Figure 4. Enriched pathway chart. The X-axis represented as Rich Factor is the number of differential proteins annotated to the Pathway divided by all the proteins identified to the Pathway. The greater the value, the larger the proportion of Pathway differential proteins. The dot size in the figure indicates the amount of differential proteins annotated to the Pathway.

[30] and ABC transporter lipoprotein *bldKB* (SCO5113) [31] are membrane proteins [32, 33] which are considered as the main carriers for energy conversion, peptide and nutrient transport. These two transporters have been shown to be involved in the transport of extracellular peptides. We predicted functional partners of SCO5477 through the online prediction website. The ABC transporter integral membrane protein *bldKA* (SCO5112), ABC transporter integral membrane protein *bldKC* (SCO5114), and ABC transporter intracellular ATPase subunit *bldKD* (SCO5115) are predicted functional partners of SCO5477. It can be further inferred that the deletion of *sco4114* gene blocked the growth of aerial mycelia by affecting the expression of *bld* system. In addition, *sco4114* gene contains TTA codon. The product of *bldA* gene, tRNA Leu UUA, is the only tRNA encoding Leu rare codon UUA in *Streptomyces* [34]. *BldA* gene participates in the regulation of genes containing Leu (UUA) at the translation level. *sco4114* gene is regulated by *bldA* gene, and knockout *sco4114* gene also affects the expression of *bld* family genes.

As a critical methyl donor, S-adenosylmethionine (SAM, SCO1476) [30, 35] which is down-regulated in our proteomic analysis, is involved in the regulation of *Streptomyces* differentiation. It can enhance the expression of oligopeptide-binding components related to ABC transporters such as *bldK* which is a well-known regulatory factor in *S. coelicolor* differentiation [36].

(c) Post-transcriptional modification

The expression of major chaperone proteins involved in the post-transcriptional modification phase is significantly down-regulated including the chaperone GroEL (SCO4296 and SCO4276)

Table 2. Pathway enrichment analysis of differential proteins.

#	Pathway	Different Proteins annotated to the pathway (146)	All Proteins annotated to the pathway (2,326)	P- value	Pathway ID
1	Ribosome	15 (10.27%)	51 (2.19%)	2.041059e-07	ko03010
2	Tuberculosis	5 (3.42%)	7 (0.3%)	1.728421e-05	ko05152
3	Citrate cycle	10 (6.85%)	35 (1.5%)	3.295983e-05	ko00020
4	RNA polymerase	3 (2.05%)	4 (0.17%)	0.0009254354	ko03020
5	2-Oxocarboxylic acid metabolism	7 (4.79%)	32 (1.38%)	0.002958451	ko01210
6	Carbon fixation in photosynthetic organisms	5 (3.42%)	17 (0.73%)	0.003042287	ko00710
7	Porphyrin and chlorophyll metabolism	8 (5.48%)	41 (1.76%)	0.003224748	ko00860
8	Biosynthesis of amino acids	18 (12.33%)	146 (6.28%)	0.003550709	ko01230
9	Carbon metabolism	19 (13.01%)	172 (7.39%)	0.009303877	ko01200
10	Methane metabolism	7 (4.79%)	43 (1.85%)	0.01584953	ko00680
11	Glyoxylate and dicarboxylate metabolism	8 (5.48%)	56 (2.41%)	0.02155483	ko00630
12	Carbon fixation pathways in prokaryotes	6 (4.11%)	36 (1.55%)	0.0224336	ko00720
13	Nicotinate and nicotinamide metabolism	4 (2.74%)	23 (0.99%)	0.05185796	ko00760
14	Cysteine and methionine metabolism	5 (3.42%)	33 (1.42%)	0.05197539	ko00270
15	Glycolysis / Gluconeogenesis	8 (5.48%)	76 (3.27%)	0.1000842	ko00010
16	Biosynthesis of secondary metabolites	31 (21.23%)	401 (17.24%)	0.1154421	ko01110
17	Biosynthesis of antibiotics	25 (17.12%)	320 (13.76%)	0.1374601	ko01130
18	Microbial metabolism in diverse environments	26 (17.81%)	346 (14.88%)	0.1805122	ko01120
19	Pyruvate metabolism	6 (4.11%)	63 (2.71%)	0.2000089	ko00620
20	Alanine, aspartate and glutamate metabolism	4 (2.74%)	38 (1.63%)	0.2126945	ko00250
21	Pyrimidine metabolism	5 (3.42%)	52 (2.24%)	0.2247328	ko00240
22	Propanoate metabolism	4 (2.74%)	42 (1.81%)	0.2683241	ko00640
23	Metabolic pathways	55 (37.67%)	820 (35.25%)	0.2920666	ko01100
24	Purine metabolism	7 (4.79%)	86 (3.7%)	0.292857	ko00230
25	Pentose phosphate pathway	4 (2.74%)	44 (1.89%)	0.2970903	ko00030
26	Two-component system	7 (4.79%)	135 (5.8%)	0.7575061	ko02020

and the chaperone DnaK (SCO3671). This is a relatively important chaperone protein in *Streptomyces*, which is involved in the activation and expression of proteins during the transformation of dormant vegetative bodies into metabolically active vegetative bodies [37]. During germination, protein synthesis rate increases while it is accompanied by the binding of DnaK to ribosomes [38]. Therefore, the down-regulation of chaperone protein may influence the synthesis of proteins needed in the aerial mycelium stage and result in the bald phenotype of the strain.

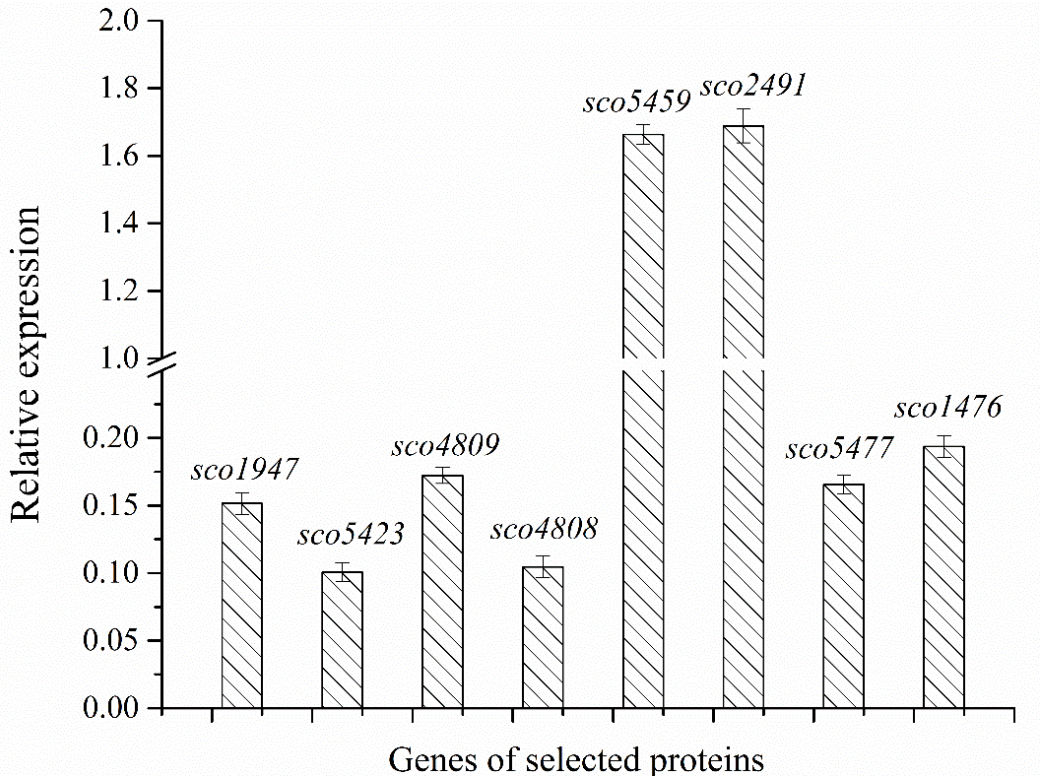

Figure 5. Relative expression levels of transcripts. Data were normalized against expression of the endogenous reference gene. To determine relative fold differences for each gene, the formula $2^{-\Delta\Delta Ct}$ was used.

(d) Ribosomal protein

During the transition of *S. coelicolor* from exponential growth phase to the sporulation period, it is accompanied by reduction in the incorporation of amino acids into proteins and changes in the pattern of protein expression [39-41]. Such a transition can be driven not only by transcription but also by structural modifications of the translational system. Eight ribosomal proteins of the small subunit (S1, S2, S3, S6, S7, S8, S10, and S15) and eight ribosomal proteins of the large subunit (L1, L5, L6, L7/L12, L10, L17, L18, and L27) are significantly down-regulated (Figure 3B). Reduction of ribosomal protein is an important signal affecting the morphological changes of *Streptomyces*.

Pathway enrichment analysis of differential proteins

It can be indicated from Figure 4 and Table 2 that the differential protein in the metabolic pathway is significantly enriched. Among the differential proteins, the majority is involved in primary metabolism including TCA cycle (6.85%), biosynthesis of amino acids (12.33%), and carbon metabolism (13.01%). 21.23% of differentially expressed proteins are involved in secondary metabolite synthesis while about 17% of proteins are involved in antibiotic synthesis.

Analysis of differential protein abundance at the transcriptional level using qRT-PCR

To compare the changes in protein abundance identified by iTRAQ related to changes at the gene transcription level, qRT-PCR analysis was performed. Eight of these proteins were selected for analysis in which the proteins were chosen according to expression levels from the iTRAQ proteomic data. Overall, our results showed that the trends in gene expression profiles from qRT-PCR were positively correlated with the iTRAQ data, which suggested that the proteomic results were of good quality (Figure 5).

Conclusion

Aerial mycelium formation and sporulation of *Streptomyces* are very important physiological processes, which require the interaction of many functional proteins and regulatory factors. SCO4114 is labeled sporulation-related protein, but its effect on sporulation has not been studied in detail, and its mechanism is completely unclear. Therefore, ⊿*sco4114* strain was constructed in this study and the effects on the production of aerial mycelium and the proteome were investigated.

It was concluded that the deletion of *sco4114* gene results in premature spores and some alteration in the proteome. Among the identified proteins, most of the proteins involved in carbon metabolism, ABC transporters, various chaperones, and ribosomal proteins were significantly down-regulated while the proteins involved in nitrogen metabolism were significantly up-regulated. *sco4114* gene contains TTA codon. The product of *bldA* gene is the only tRNA which encodes Leu rare codon UUA in *Streptomyces*. Therefore, SCO4114 must be regulated by *bldA* gene. At the same time, carbon metabolism and ABC transporters were closely related to *bld* cascades. We speculated that down-regulated carbon metabolism blocked the first step of signal cascade by reducing the expression of *bldK*. The *bldB* gene product might be the protein that interacts with glucose kinase [42].

SCO5477 contains cys residue, which is a potential target for ADP ribosylation. Cys ADP ribosylation can interfere with the transportation and location of binding proteins. SCO5477 may influence the formation of aerial mycelia by affecting the intracellular transportation and localization of SCO4114 protein, which may be further regulated by *bldKB* or participate in the regulation of *bldKB* expression. Therefore, we further speculate that SCO4114 participates in the formation of aerial hyphae through the following mechanisms: the structure of N-terminal signal peptide of SCO4114 protein is guided by chaperone in cytoplasm, and it is motivated by ATP to move to a specific site on the membrane, that is, SCO5477 protein. After binding with SCO5477, the structure of oligopeptide binding protein changes, which makes SCO5477 secrete or bind to specific substances. This substance will affect the expression of *bldKB*. Reducing the number of *bldKB* on the membrane may result in not receiving enough differentiation signal peptide, and thus hindering the formation of aerial mycelium. Moreover, it would also be a good proposal in the future investigation to verify whether there is a direct interaction between SCO4114 and SCO5477.

The oligopeptide binding proteins in ABC transport system were further affected because many significantly down-regulated ABC transporters also belong to the *bld* system. Therefore, the production of aerial mycelium might be affected by *bld* cascade. The comparative proteomic analysis of strain ⊿*sco4114* laid the foundation for us to find the potential binding proteins with SCO4114 protein or protein which directly regulate SCO4114.

Acknowledgement

This study was financially supported by the National Key Research and Development Program of China (2017YFD0201400), the National Natural Science Foundation of China (31370091), and the Funds for Creative Research Groups of China (21621004).

References

1. Dworkin M: Prokaryotic Life Cycles. Prokaryotes. Volume 2. Edited by Dworkin M. New York: Springer; 2006:140-166.
2. Angel M, Marisol F, Jesús S. 2005. A death round affecting a young compartmentalized mycelium precedes aerial mycelium dismantling in confluent surface cultures of Streptomyces antibioticus. Microbiology +. 151:36-89.

3. Manteca A, Fernandez M, Sanchez J. 2005. Mycelium development in Streptomyces antibioticus ATCC11891 occurs in an orderly pattern which determines multiphase growth curves. BMC Microbiol. 5: 51-51.
4. Manteca A, Fernandez M, Sanchez J. 2006. Cytological and biochemical evidence for an early cell dismantling event in surface cultures of Streptomyces antibioticus. Res Microbiol. 157:143-152.
5. Angel M, Dennis C, Carmen LI, et al. 2010. Aerial hyphae in surface cultures of Streptomyces lividans and Streptomyces coelicolor originate from viable segments surviving an early programmed cell death event. FEMS Microbiol Lett. 274:118-125.
6. Angel M, Jesus S. Streptomyces development in colonies and soils. 2009. Appl Environ Microb. 75:2920.
7. Manteca A, Alvarez R, Salazar N, et al. 2008. Mycelium differentiation and antibiotic production in submerged cultures of Streptomyces coelicolor. Appl Environ Microb. 74:3877-3886.
8. Angel M, Marisol F, Jesús S. 2005. A death round affecting a young compartmentalized mycelium precedes aerial mycelium dismantling in confluent surface cultures of Streptomyces antibioticus. Microbiology +. 151:3689.
9. Keleman GH, Buttner MJ. 1999. Initiation of aerial mycelium formation in Streptomyces. Curr Opin Microbiol. 2:656.
10. Willey JM, Andrew W, Shinya K, et al. 2010. Morphogenetic surfactants and their role in the formation of aerial hyphae in Streptomyces coelicolor. Mol Microbiol. 59:731-742.
11. Hindra, Moody MJ, Jones SE, et al. 1932. Complex intra-operonic dynamics mediated by a small RNA in Streptomyces coelicolor. PLoS One. 9:85-86.
12. Shinya K, Hudson ME, Durrant MC, et al. 2004. The SapB morphogen is a lantibiotic-like peptide derived from the product of the developmental gene ramS in Streptomyces coelicolor. P Natl ACAD Sci USA. 101:11448-11453.
13. Yinhua L, Juanmei H, Hong Z, et al. 2011. An orphan histidine kinase, OhkA, regulates both secondary metabolism and morphological differentiation in Streptomyces coelicolor. J Bacteriol. 193:3020-3032.
14. Elliot MA, Nitsara K, Jianqiang H, et al. 2003. The chaplins: a family of hydrophobic cell-surface proteins involved in aerial mycelium formation in Streptomyces coelicolor. Genes Dev. 17:1727-1740.
15. Liu S, Wu Q, Zhang J, et al. 2012. Enhanced epsilon-poly-L-lysine production from Streptomyces ahygroscopicus by a combination of cell immobilization and in situ adsorption. World J Microb Biot. 22:1218.
16. Chang JK, Yong KC, Chun GT, et al. 2010. Continuous Culture of Immobilized Streptomyces Cells for Kasugamycin Production. Biotechnol Progr. 17:453-461.
17. Babcock MJ, Kendrick KE. 1988. Cloning of DNA involved in sporulation of Streptomyces griseus. J Bacteriol. 170:2802-2808.
18. Mccue LA, Kwak J, Wang J, et al. 1996. Analysis of a gene that suppresses the morphological defect of bald mutants of Streptomyces griseus. J Bacteriol. 178:2867-2875.
19. Intra B, Euanorasetr J, Nihira T, et al. 2016. Characterization of a gamma-butyrolactone synthetase gene homologue (stcA) involved in bafilomycin production and aerial mycelium formation in Streptomyces sp. SBI034. Appl Microbiol Biot. 100:2749-2760.
20. Wang H, Wei H, Tang L, et al. 2018. A proteomics of gills approach to understanding salinity adaptation of Scylla paramamosain. Gene. 677:119-131.
21. Sun L, Xu D, Xu Q, et al. 2017. iTRAQ reveals proteomic changes during intestine regeneration in the sea cucumber Apostichopus japonicus. Comp Biochem Phys D. 22:39-49.
22. Bradford MM. 1976. A Rapid Method for the Quantitation of Microgram Quantities of Protein Utilizing the Principle of Protein-Dye Binding. Anal Biochem. 72:248–254.
23. Shi CH, Rubel C, Soss SE, et al. 2018. Disrupted structure and aberrant function of CHIP mediates the loss of motor and cognitive function in preclinical models of SCAR16. PLOS Genet. 14:e1007664.
24. Sachon E, Mohammed S, Bache N, et al. 2010. Phosphopeptide quantitation using amine-reactive isobaric tagging reagents and tandem mass spectrometry: application to proteins isolated by gel electrophoresis. Rapid Commun Mass SP. 20:1127-1134.
25. Bo W, Ruo Z, Qiang F, et al. 2015. IQuant: an automated pipeline for quantitative proteomics based upon isobaric tags. Proteomics. 14:2280-2285.
26. Savitski MM, Wilhelm M, Hahne H, et al. 2015. A Scalable Approach for Protein False Discovery Rate Estimation in Large Proteomic Data Sets. Mol Cell Proteomics. 14:2394.
27. Romero-Rodríguez A, Rocha D, Ruiz-Villafán B, et al. 2017. Carbon catabolite regulation in Streptomyces: new insights and lessons learned. World J Microbiol Biotechnol. 33:162.
28. Goerke B, Stulke J. 2008. Carbon catabolite repression in bacteria: many ways to make the most out of nutrients. Nat Rev Microbiol. 6:613.
29. Yang HW, Cheng YW, Zhang JH. 2009. Progress of Regulatory Mechanism of Morphological Differentiation and Secondary Metabolism in Streptomyces. Journal of Mianyang Normal University. 28(11):63-68.
30. Shin SK, Park HS, Kwon HJ, et al. 2007. Genetic characterization of two S-adenosylmethionine-induced ABC transporters reveals their roles in modulations of secondary metabolism and sporulation in Streptomyces coelicolor M145. J Microbiol Biotechnol. 17:1818-1825.
31. Li F, Liang J, Wang W, et al. 2014. Analysis of Streptomyces coelicolor membrane proteome using

two-dimensional native/native and native/sodium dodecyl sulfate gel electrophoresis. Anal Biochem. 465:148-155.

32. Nodwell J.R, Losick R. 1998. Purification of an Extracellular Signaling Molecule Involved in Production of Aerial Mycelium by Streptomyces coelicolor. J Bacteriol. 180:1334.
33. Adán C, Angela F, Mauricio S, et al. 2011. Interaction of SCO2127 with BldKB and its possible connection to carbon catabolite regulation of morphological differentiation in Streptomyces coelicolor. Appl Microbiol Biotechnol. 89:799-806.
34. Stefanie H, Andreas B. 2015. The Gene bldA, a regulator of morphological differentiation and antibiotic production in streptomyces. Arch Pharm. 348:455-462.
35. Meng LZ, Yang SH, Palaniyandi SA, et al. 2011. Phosphoprotein affinity purification identifies proteins involved in S-adenosyl-L-methionine-induced enhancement of antibiotic production in Streptomyces coelicolor. J Antibiot. 64:97-101.
36. Park HS, Shin SK, Yang YY, et al. 2010. Accumulationof S-adenosylmethionine induced oligopeptide transporters including BldK to regulate differentiation events in Streptomyces coelicolor M145. Fems Microbilo Lett. 249:199-206.
37. Jan B, Petr H, Jakub A, et al. 2010. Activation and expression of proteins during synchronous germination of aerial spores of Streptomyces granaticolor. Proteomics. 4:3864-3880.
38. Akhter Y, Thakur S. 2017. Targets of ubiquitin like system in mycobacteria and related actinobacterial species. Microbilo Res. 204:9-29.
39. Mikulík K, Bobek J, Ziková A, et al. 2011. Phosphorylation of ribosomal proteins influences subunit association and translation of poly (U) in Streptomyces coelicolor. Mol Biosyst. 7:817-823.
40. Bobek J, Halada P, Angelis J, et al. 2010. Activation and expression of proteins during synchronous germination of aerial spores of Streptomyces granaticolor. Proteomics. 4:3864-3880.
41. Piette A, Derouaux A, Gerkens P, et al. 2005. From dormant to germinating spores of Streptomyces coelicolor A3(2): new perspectives from the crp null mutant. J Proteome Res. 4:1699.
42. Pope MK, Green BD, Westpheling J. 2010. The bld mutants of Streptomyces coelicolor are defective inthe regulation of carbon utilization, morphogenesis and cell--cell signaling. Mol Microbiol. 19:747-756.